Elastomers and Composites
Vol. 60, No. 2, pp. 77~84 (June 2025)

Print ISSN 2092-9676/Online ISSN 2288-7725
DOI: https://doi.org/10.7473/EC.2025.60.2.77

Synthesis of Nickel Zeolitic Imidazolate Framework/Carbon Nanotube Nanocomposite as a Catalyst for Reduction of Nitroaromatic Compounds

Sugyeong Jeon[*], Jeong Won Ko[**], and Weon Bae Ko[*,*,†]**

[*]*Department of Convergence Science, Graduate School of Sahmyook University, Seoul 01795, Republic of Korea*
[**]*Department of Animal Resources Science, Sahmyook University, Seoul 01795, Republic of Korea*
[***]*Department of Chemistry, Sahmyook University, Seoul 01795, Republic of Korea*

(Received April 16, 2025, Revised May 11, 2025, Accepted June 30, 2025)

Abstract: A nickel zeolitic imidazolate framework/carbon nanotube (Ni-ZIF/CNT) nanocomposite was synthesized by reacting nickel(II) nitrate hexahydrate with 2-methylimidazole and carbon nanotube. Its morphology and structure were characterized using scanning electron microscopy, powder X-ray diffraction, Fourier transform infrared spectroscopy, and Raman spectroscopy. The catalytic activity of the nanocomposite for the reduction of nitroaromatic compounds, including 4-nitroaniline and 4-nitrophenetole, was monitored using an ultraviolet-visible spectrophotometer. The kinetics of the catalytic reduction of nitroaromatic compounds followed a pseudo-first-order reaction rate law. The Ni-ZIF/CNT nanocomposite prepared with 15 wt.% CNT exhibited the highest catalytic performance in the reduction of nitroaromatic compounds. The rate constants (k) for the reduction of 4-nitroaniline and 4-nitrophenetole by the Ni-ZIF/CNT nanocomposite containing 15 wt.% CNTs were 0.1930 and 0.1106, respectively.

Keywords: Ni-ZIF/CNT nanocomposite, reduction of nitroaromatic compounds, kinetics, pseudo-first order reaction

Introduction

Nitroaromatic compounds are widely used in many industries.[1,2] However, they are toxic, mutagenic, and carcinogenic; therefore, considerable research is being conducted on pollutant removal.[3] Methods for removing nitroaromatic compounds, which are contaminants, include physicochemical, adsorption, and microbial methods.[4-6] The most widely used method is the hydrogenation of nitroaromatic compounds through reduction of its nitro group to an amine group.[7-9] Also, the catalytic hydrogenation of nitroaromatic compounds has been widely used in numerous industries for use as an intermediate in the synthesis of oxidizing agents, drugs, and pesticides.[10-12]

Metal organic frameworks (MOFs) have attracted increasing attention in past decades because of their high specific surface area, adjustable porosity, and variable structures.[13] Since zeolitic imidazolate framework (ZIF) is composed of tetrahedral coordinated transition metal ions and imidazole linker, it has a structure similar to zeolite. ZIF can be used as porous nanostructures for organic semiconductor catalysts.[14] A nickel-based imidazolate framework was prepared using Ni^{2+} ions as the central metal ion and a methanol solution containing 2-methylimidazole.[15-19] Nickel, zinc, and cobalt can be nucleated with an imidazole at ambient temperature to form typical ZIF. The overall yield product of Ni-ZIF is very low.[19] Nickel is a magnetic and ferromagnetic element like Co and Fe. In addition, nickel is not easily oxidized and resistant to corrosion. Ni-ZIF efficiently combines these advantages and can be used as efficient catalytic materials.[20,21]

Carbon nanotube (CNT) has excellent electronic, mechanical, and structural properties. Due to these properties CNT is widely used in gas storage, catalysis, and energy storage applications.[22] CNT-based nanohybrid materials exhibit the synergistic effect of two components that combine the advantages of their high specific surface area, small size, and hollow structure.[23] The hybrid nanocomposite of Ni-ZIF with CNT was more efficiently reduces nitroaromatic compounds than a single MOF catalyst.[24]

In this study, Ni-ZIF/CNT nanocomposite was synthesized using nickel nitrate hexahydrate and 2-methylimidazole at 1:6 molar ratio. Methanol was used as the solvent. The

[†]Corresponding author E-mail: kowb@syu.ac.kr

hybrid nanocomposite was synthesized at six different CNT concentrations (5, 10, 15, 20, 25, and 50 wt.%) are synthesized. The catalytic activity of the Ni-ZIF/CNT nanocomposite in the reduction of nitroaromatic compounds, including 4-nitroaniline and 4-nitrophenetole, was investigated. The reduction efficiency of the nitroaromatic compounds in the nanocomposite as a catalyst which was composed of Ni-ZIF/CNT was compared based on the CNT contents.

Experimental

1. Materials

This study was performed using nickel nitrate hexahydrate ($Ni(NO_3)_2 \cdot 6H_2O$, 98%; Samchun pure chemicals), 2-methylimidazole (99%, $C_4H_6N_2$; Alfa Aesar), polyvinylpyrrolidone (PVP, average mol wt. 10,000; Sigma-Aldrich), carbon nanotube (CNT; Carbon nano-material Technology Co. Ltd, Republic of Korea), methanol (99.5%, CH_3OH; Daejung chemicals), 4-nitrophenetole (97.0%, $C_8H_9NO_3$; Sigma-Aldrich), 4-nitroaniline (≥99%, $C_6H_6N_2O_2$; Sigma-Aldrich), and sodium borohydride ($NaBH_4$; Samchun pure chemicals). All chemicals were used without further purification.

2. Instruments

The crystalline properties of the synthesized Ni-ZIF/CNT nanocomposite were investigated by powder X-ray diffraction (XRD, Bruker, D8 Advance, Germany) analysis with Cu-Kα radiation (λ=1.541 nm) within a 2θ range of 10–60°. The Ni-ZIF/CNT nanocomposite was confirmed using Raman spectroscopy at a wavelength of 532 nm (BWTEK i-Raman Plus, USA). The morphology of the synthesized catalyst was observed using scanning electron microscopy (SEM, TESCAN MIRA 3, Czech Republic) at an acceleration voltage of 15 kV. The functional groups of the catalyst were analyzed using Fourier-transform infrared spectroscopy (FT-IR, Thermo Fisher Scientific Nicolet Continuum IR Microscope, USA). The catalytic activity of the Ni-ZIF/CNT nanocomposite was confirmed by UV-vis spectroscopy (Lambda 365, Perkin Elmer, USA).

3. Synthesis of Ni-ZIF nanoparticles

To produce the Ni-ZIF nanoparticles, 0.582 g nickel nitrate hexahydrate ($Ni(NO_3)_2 \cdot 6H_2O$) and 0.985 g 2-methylimidazole were dissolved in 10 ml methanol, respectively. The two solutions were then mixed and stirred for 30 min. Subsequently, the solution was heated at 60ºC for 12 h. Finally, the yellowish precipitate was collected by centrifugation at 3600 rpm for 30 min and washed several times with methanol until all the unbound metal ions and organic ligands were removed. The final product after washing was dried at 60ºC for overnight.

4. Synthesis of Ni-ZIF/CNT nanocomposite

To synthesize the Ni-ZIF/CNT nanocomposite, 1-10 mg of CNT and 0.1 g of polyvinylpyrrolidone (PVP) were added to 10 ml of methanol, sonicated to disperse for 1 h, and then stirred for 2 h. After sonication, 0.985 g of 2-methylimidazole was added to the CNT solution and stirred for 0.5 h, and then 10 ml of methanol solution containing 0.582 g of nickel nitrate hexahydrate ($Ni(NO_3)_2 \cdot 6H_2O$) was added to the dispersion. The mixture was stirred at 60ºC for 12 h. The precipitate was washed several times with methanol, collected by centrifugation, and then dried at 60ºC.

5. Reduction of nitroaromatic compounds

The catalytic reduction of 4-nitroaniline and 4-nitrophenetole using Ni-ZIF/CNT nanocomposite catalyst was performed in the presence of $NaBH_4$. The initial concentrations of the 4-nitroaniline and 4-nitrophenetole solution were 0.05 mM. Sodium borohydride was used as a reducing agent in the reduction reaction. 2.7 mM $NaBH_4$ was added to 0.05 mM the nitroaromatic solution. Then the 0.2 g/L catalyst was added to the nitroaromatic solution and stirred using a magnetic stirrer. The catalytic reduction of nitroaromatic compounds to their corresponding aromatic amines was monitored at 2 min intervals using UV-vis spectroscopy.

In the presence of $NaBH_4$, 4-nitroaniline solution shows a maximum peak at λ=381 nm in UV-vis spectrum. During the reduction, the absorbance at 381 nm gradually decreased, and the absorbance band of the new peak at 305 nm, corresponding to *p*-phenylenediamine, increased. The UV-vis spectrum of the 4-nitrophenetole solution containing excess $NaBH_4$ showed a characteristic absorption band at 318 nm. As the reaction progressed, the absorbance band at 318 nm gradually decreased, and a new absorption wavelength appeared at 290 nm due to the production of *p*-phenetidine.

Results and Discussion

1. Characterization of Ni-ZIF/CNT nanocomposite

In Figure 1, the FT-IR spectrum of the Ni-ZIF/CNT nanocomposite showed absorption peaks representing symmetric and asymmetric vibrations. The peak at 473 cm^{-1} represents Ni-N vibrations. This peak value is attributed to the coordinative bond between Ni^{2+} and 2-methylimidazole and confirm the formation of Ni-ZIF nanoparticles. In Ni-ZIF nanoparticles, the peak at 1462 cm^{-1} was assigned to the CN stretching vibrations. The bands at 1000 cm^{-1}, 1145 cm^{-1} and 1308 cm^{-1} were associated with the in-plane bending of the ring, and the bands below 736 cm^{-1} were attributed to the out-of-plane bending of 2-methylimidazole. The FT-IR spectrum of the Ni-ZIF/CNT nanocomposite was similar to that of Ni-ZIF nanoparticles in Figure 1.

X-ray diffraction analysis was performed to investigate the structure of Ni-ZIF nanoparticles. The XRD patterns of the Ni-ZIF nanoparticles were shown in Figure 2(a). Unlike Zn-ZIF and Co-ZIF, the as-synthesized Ni-ZIF nanoparticles lacked of characteristic high-intensity peaks, indicating that the structure was not crystalline. The diffraction peak at approximately 13.9° in Ni-ZIF nanoparticles corresponded to the (211) crystal plane.[25] The XRD peak of CNT was observed at 26°, corresponding to the (002) plane. In Figure 2, CNT did not has a significant effect on the XRD peaks of Ni-ZIF/CNT nanocomposite. This is because of the CNT overlaps with the peak of Ni-ZIF nanoparticles.[26,27]

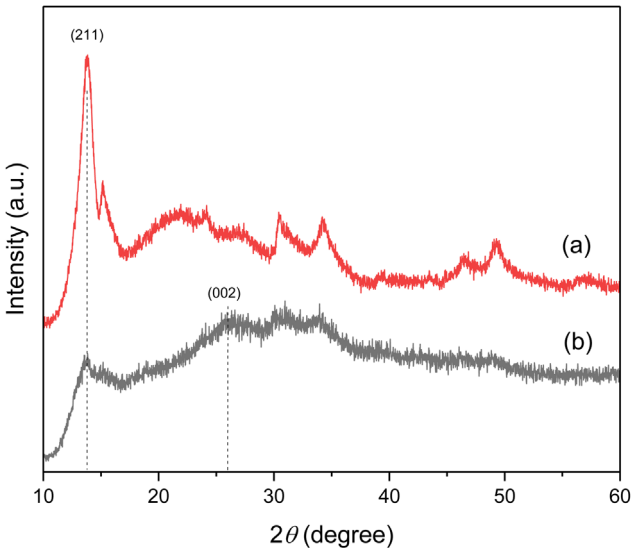

Figure 2. XRD patterns of synthesized (a) Ni-ZIF nanoparticles and (b) Ni-ZIF/CNT nanocomposite.

The Raman spectra of the Ni-ZIF/CNT nanocomposite are shown in Figure 3. In the Raman spectra of the CNT, the peaks at 1339 cm^{-1}, 1576 cm^{-1}, and 2694 cm^{-1} correspond to the D, G and 2D bands of the CNT, respectively. The bands at 697, 1033, 1191, and 1465 cm^{-1} in the Raman spectra are related to the N-H wagging mode and the C-H wagging mode of 2-methylimidazole in Ni-ZIF nanoparticles. These two bands suggest that the CNT content increases in the Ni-ZIF/CNT nanocomposite. In the Ni-ZIF/CNT nancomposite,

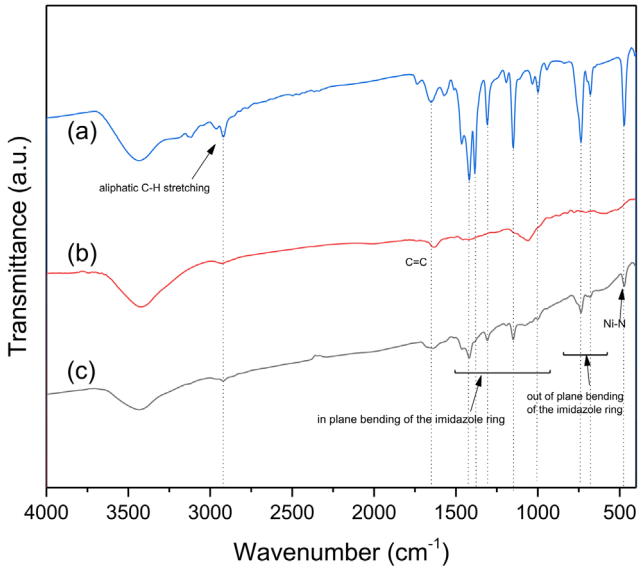

Figure 1. FT-IR spectra of synthesized (a) Ni-ZIF nanoparticles (b) CNT and (c) Ni-ZIF/CNT nanocomposite.

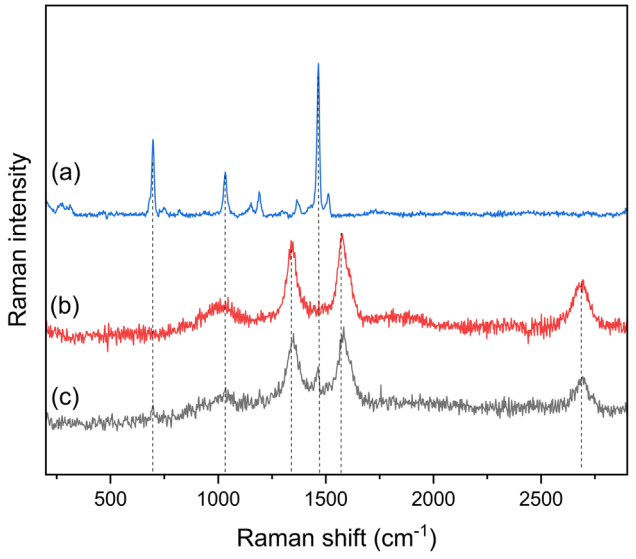

Figure 3. Raman spectra of synthesized (a) Ni-ZIF nanoparticles (b) CNT and (c) Ni-ZIF/CNT nanocomposite.

the D and G bands of CNT were confirmed to shift to 1350 cm^{-1} and 1583 cm^{-1}, and the peaks of 1465 cm^{-1} and 697 cm^{-1} attributed to the Ni-ZIF nanoparticles were confirmed.

Figure 4 showed the morphologies of Ni-ZIF nanoparticles and Ni-ZIF/CNT nanocomposite, measured by SEM. Nano-flower-like structures are observed in the Ni-ZIF nanoparticles. The CNT appeared to surround the Ni-ZIF nanoparticles while the crystal structure of the Ni-ZIF nanoparticles was maintained.

The UV-vis absorption spectra of Ni-ZIF and Ni-ZIF/CNT nanocomposite were shown in Figure 5. These spectra showed two absorption bands at 240 and 280 nm. As shown in Equation (1), the energy of bandgap was calculated using the following Tauc plot equation:

$$\alpha h\nu = A[h\nu - E_g]^k \quad (1)$$

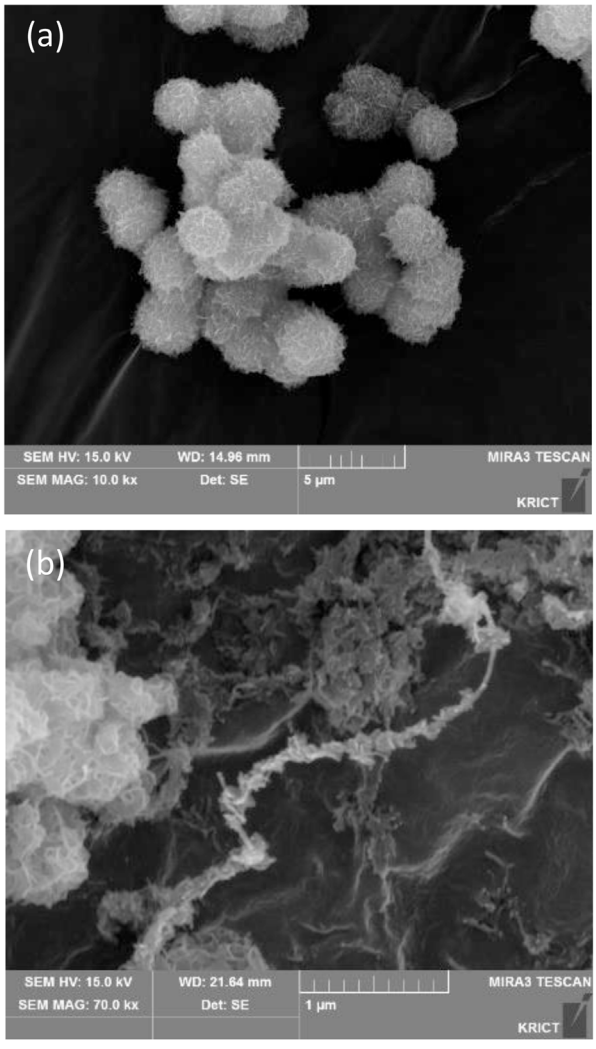

Figure 4. SEM images of synthesized (a) Ni-ZIF nanoparticles and (b) Ni-ZIF/CNT nanocomposite.

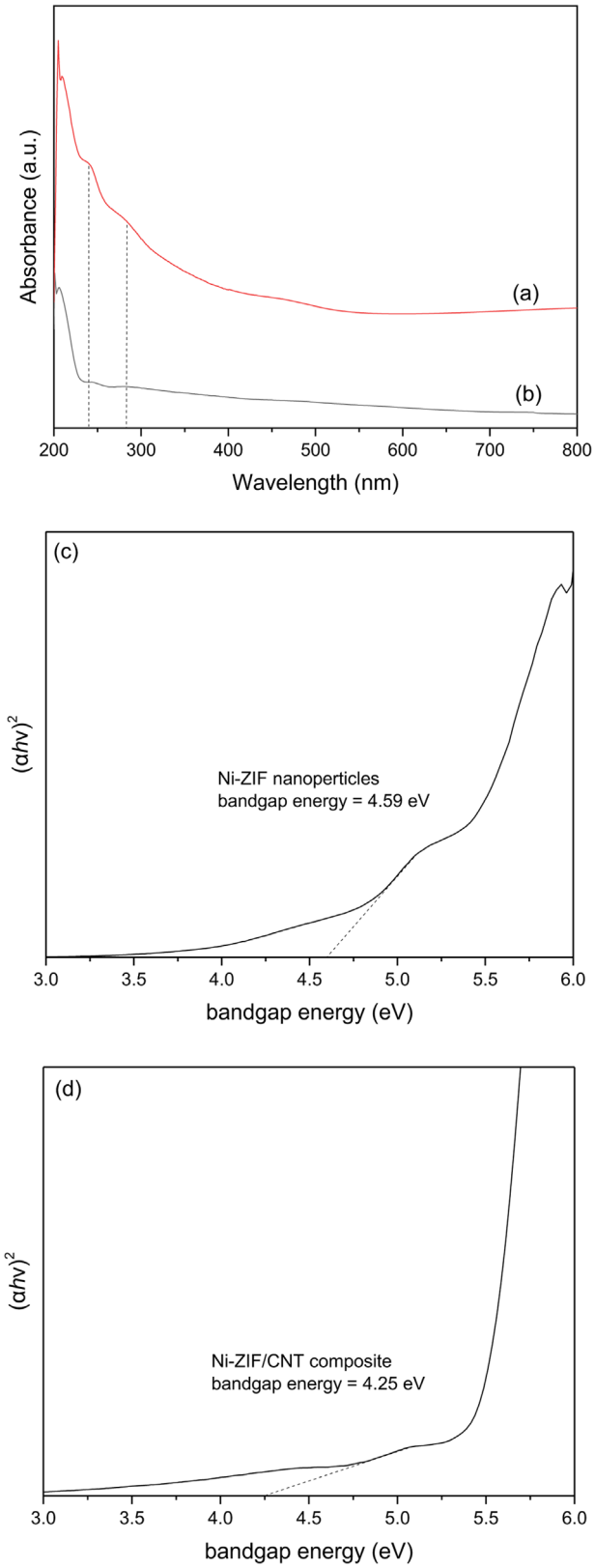

Figure 5. UV-vis spectra of the (a) Ni-ZIF nanoparticles and (b) Ni-ZIF/CNT nanocomposite and Tauc's plot for the bandgap energy of the (c) Ni-ZIF nanoparticles and (d) Ni-ZIF/CNT nanocomposite.

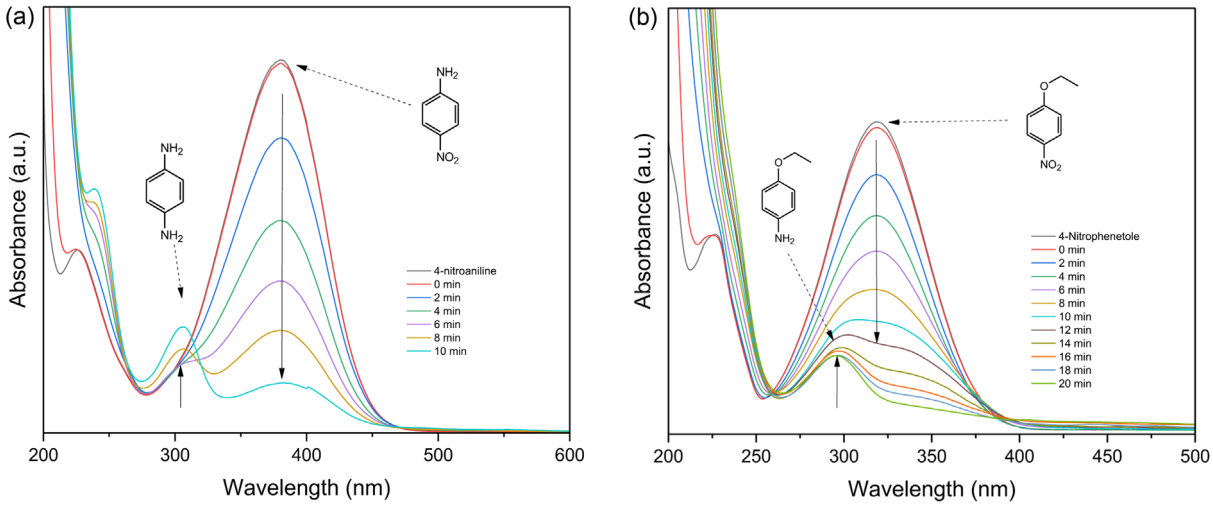

Figure 6. UV-vis spectra of reduction of (a) 4-nitroaniline and (b) 4-nitrophenetole in the presence of $NaBH_4$ with Ni-ZIF/CNT nanocomposite as a catalyst.

where α is the absorption coefficient, h is Plank's constant, v is the frequency of the light, A is a characteristic constant of the semiconductor, E_g is the apparent optical band gap of the material, and k is a constant related to the type of electronic transition for indirect allowed transition (k = 2). The bandgap energy for Ni-ZIF nanoparticles and Ni-ZIF/CNT nanocomposite were 4.59 and 4.25 eV, respectively.

2. Catalytic application of Ni-ZIF/CNT nanocomposite for the reduction of nitroaromatic compounds

To improve catalytic efficiency, Ni-ZIF/CNT nanocomposite was prepared by adding different amounts of CNT. The hybrid nanocomposite catalyst showed higher catalytic activity for the reduction of nitroaromatic compounds than the Ni-ZIF nanoparticles, itself.

The catalytic activity of the synthesized Ni-ZIF/CNT nanocomposite was investigated by measuring the degree of reducing nitroaromatic compounds, as were shown in Figure 6. The reduction rate of nitroaromatic compounds was more increased for 4-nitroaniline than 4-nitrophenetole using Ni-ZIF nanoparticles placed on CNT as a catalyst. It was taken 10 min for 4-nitroaniline and 20 min for 4-nitrophenetole to complete the reductive reaction.[7,8]

3. Kinetics study for catalytic reduction of nitroaromatic compounds

For the catalytic reduction of nitroaromatic compounds, hydride (H^-) ions generated from $NaBH_4$ were used as the main reducing agent.[8,15] The reduction rate was calculated from the reaction rate equation for the catalytic reduction of nitroaromatic compounds, using $NaBH_4$ as the reducing agent. Since the concentration of $NaBH_4$ is very high compared to the concentration of nitroaromatic compounds in the reaction, it can be assumed that the concentration of $NaBH_4$ remains constant during the reaction. For this reason, the reduction equation follows a pseudo-first-order reaction rate law.

$$\frac{dc}{dt} = -kC \tag{2}$$

$$ln\left(\frac{C}{C_0}\right) = -kt \tag{3}$$

where C is the initial concentration of the reactant, k is the first-order rate constant, and t is reaction time.

The rate constants of the reduction by the catalyst with different CNT content were listed in Table 1. Figure 7 showed the reduction rates by the Ni-ZIF/CNT nanocomposite with different CNT content. The Ni-ZIF/CNT nanocomposite exhibited the fastest reduction rate when they contained 15 wt.% content of CNT. During the reduction, 4-nitroaniline was reduced by 86.5% in 10 min and 4-nitrophenetole was reduced by 87.9% in 20 min. When the Ni-ZIF/CNT nanocomposite containing 15 wt.% of CNT nanoparticles was used as a catalyst, the reduction rate of 4-nitroaniline was three times faster, and the reduction rate of 4-nitrophenetole was two times faster than when Ni-ZIF nanoparticles were

Table 1. Change in the Catalytic Reduction Rate Constants and Reduction Efficiency of 4-Nitroaniline and 4-Nitrophenetole with Various Weight Ratios of CNT in Ni-ZIF/CNT Nanocomposite.

Compound	CNT contents (wt.%)	k (min^{-1})	Reduction efficiency (%)
4-nitroaniline	0	0.0788	48.4
	5	0.1165	61.4
	10	0.1342	70.7
	15	0.1930	86.5
	20	0.1473	76.7
	25	0.1241	66.8
	50	0.1388	71.8
4-nitrophenetole	0	0.0518	65.4
	5	0.0606	71.6
	10	0.0706	74.4
	15	0.1106	87.9
	20	0.0754	77.4
	25	0.0688	76.7
	50	0.0605	71.2

used as catalyst. In addition, the rate of the reduction reaction decreased when the CNT nanoparticle content exceeded 15 wt.%.

The catalytic activity for the reductive reaction is observed higher 4-nitroaniline than 4-nitrophenetole. When an electron donating group is present in the compound, the inductive effect increases electron density, which can accelerate the reduction reaction. Since the $-NH_2$ groups has a stronger inductive effect than the $-OCH_2CH_3$ groups, the reductive reaction of 4-nitroaniline proceeds more rapidly.[28]

4. Mechanism for the reduction of nitroaromatic compounds using Ni-ZIF/CNT nanocomposite catalyst

In the catalytic reduction, $NaBH_4$ acts as electron donor and hydrogen source, and the Ni-ZIF nanoparticles are an electron transfer mediator that transfers electron from BH_4^- ions to nitroaromatic compounds. On the catalyst surface, BH_4^- ions and hydrogen species of nitroaromatic compounds are simultaneously adsorbed, and the amino compounds were formed due to reaction between the adsorbed species.

Conclusions

Catalytic reduction of 4-nitroaniline and 4-nitrophenetole was performed using the Ni-ZIF/CNT nanocomposite as a catalyst in the presence of $NaBH_4$. The hybrid nanocomposite catalyst showed higher catalytic activity than Ni-ZIF nanoparticles, for the reduction of nitroaromatic compounds. Kinetics study of catalytic reduction of nitroaromatic compounds followed a pseudo-first-order reaction rate law. At constant concentrations of $NaBH_4$ and the catalyst, 4-nitroaniline was reduced faster than 4-nitrophenetole. The catalyst prepared using the Ni-ZIF/CNT nanocomposite with 15 wt.% CNT exhibited the highest catalytic performance for the reductive reaction of 4-nitroaniline and 4-nitrophenetole. The reduction rate constants (k) for 4-nitroaniline and

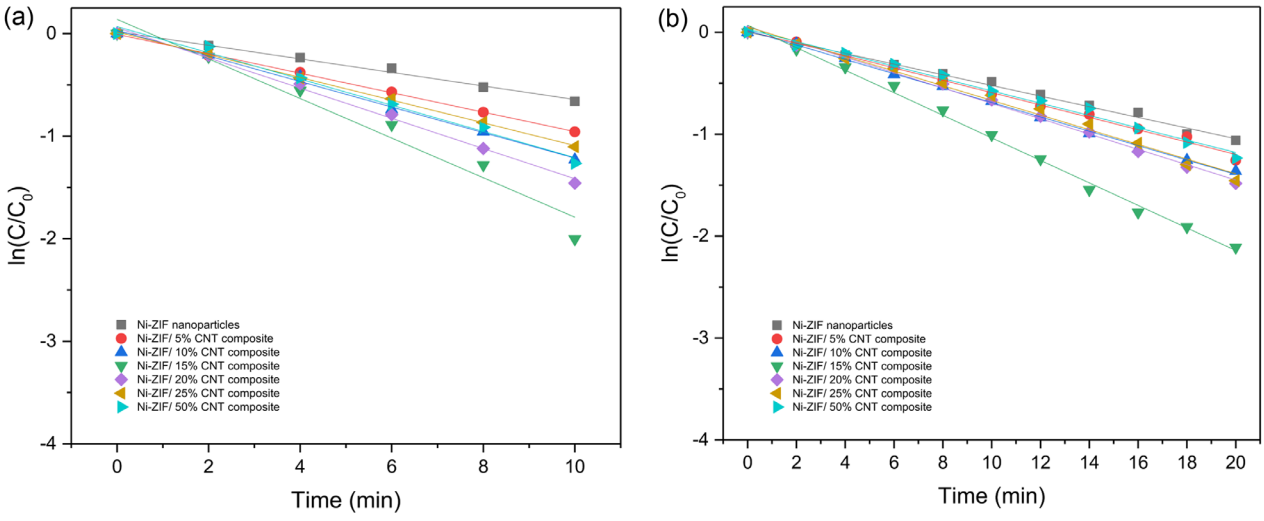

Figure 7. Kinetics study of reduction of (a) 4-nitroaniline and (b) 4-nitrophenetole in the presence of $NaBH_4$ with Ni-ZIF/CNT nanocomposite as a catalyst.

4-nitrophenetole in the Ni-ZIF/CNT nanocomposite with a 15 wt.% CNT nanoparticles ratio were 0.1930 and 0.1106, respectively.

Acknowledgements

This work was supported by Research Foundation of Sahmyook University in 2024.

Conflict of Interest: The authors declare that there is no conflict of interest.

References

1. J. Tiwari, P. Tarale, S. Sivanesan, and A. Bafana, "Environmental persistence, hazard, and mitigation challenges of nitroaromatic compounds", *Environ. Sci. Pollut. Res.*, **26**, 28650 (2019).
2. M. I. Din, R. Khalid, Z. Hussain, J. Najeeb, A. Sahrif, A. Intisar, and E. Ahmed, "Critical review on the chemical reduction of nitroaniline", *RSC Adv.*, **10**, 19041 (2020).
3. P. Kovacic and R. Somanathan, "Nitroaromatic compounds: Environmental toxicity, carcinogenicity, mutagenicity, therapy and mechanism", *J. Appl. Toxicol.*, **34**, 810 (2014).
4. G. John, S. Priyadarshini, H. Mohan, B. T. Oh, M. Navaneethan, and P. J. Jesuraj, "Unleashing the room temperature boronization: Blooming of Ni-ZIF nanobuds for efficient photo/electro catalysis of water", *Chemosphere*, **346**, 140574 (2024).
5. S. Dutta, B. Gupta, S. K. Srivastava, and A. K. Gupta, "Recent advances on the removal of dyes from wastewater using various adsorbents: A critical review", *Mater. Adv.*, **2**, 4497 (2021).
6. C. L. Zhang et al., "Recent advances in nitroaromatic pollutants bioreduction by electroactive bacteria", *Process Biochem.*, **70**, 129 (2018).
7. K. Morikawa, Y. Masubuchi, Y. Shchipunov, and A. Zinchenko, "DNA-chitosan hydrogels: Formation, properties, and functionalization with catalytic nanoparticles", *ACS Appl. Bio Mater.*, **4**, 1823 (2021).
8. M. A. Bhosale, D. R. Chenna, and B. M. Bhanage, "Ultrasound assisted synthesis of gold nanoparticles as an efficient catalyst for reduction of various nitro compounds", *ChemistrySelect*, **2**, 1225 (2017).
9. V. Malik and S. Uma, "Effective catalytic reduction of aromatic nitrocompounds using mineral beyerite, $CaBi_2O_2(CO_3)_2$", *J. Environ. Chem. Eng.*, **6**, 4755 (2018).
10. M. M. Mohamed and H. El-Farsy, "Rapid reduction of nitroarenes photocatalyzed by an innovative Mn_3O_4/α-Ag_2WO_4 nanoparticles", *Sci. Rep.*, **10**, 21495 (2020).
11. K. Shanmugaraj, T. M. Bustamante, C. H. Campos, and C. C. Torres, "Liquid phase hydrogenation of pharmaceutical interest nitroarenes over gold-supported alumina nanowires catalysts", *Materials*, **13**, 925 (2020).
12. S. Naghash-Hamed, N. Arsalani, and S. B. Mousavi, "The catalytic reduction of nitroanilines using synthesized $CuFe_2O_4$ nanoparticles in an aqueous medium", *ChemistryOpen*, **11**, e202200156 (2022).
13. D. Xu, J. Ke, H. Liu, Y. Bi, and J. Liu, "Preserving 3D Ni-ZIF nanostructure to construct NiS_2/N, S co-doped porous carbon for synergistically enhanced sustainable photo/electrocatalytic hydrogen evolution", *SSRN Preprint*, Apr. (2023).
14. Y. Z. Chen, R. Zhang, L. Jiao, and H. L. Jiang, "Metal–organic framework-derived porous materials for catalysis", *Coord. Chem. Rev.*, **362**, 1 (2018).
15. D. Formenti, F. Ferretti, F. K. Scharnagl, and M. Beller, "Reduction of nitro compounds using 3d-non-noble metal catalysts", *Chem. Rev.*, **119**, 2611 (2019).
16. J. Ba, H. Cheng, Z. Li, X. Yu, A. Song, C. Xu, D. Fan, and S. Jin, "Evolutionary mechanism of Ni-ZIF/CdS calcination for efficient photocatalytic hydrogen evolution", *J. Catal.*, **414**, 319 (2022).
17. C. W. Tsai, R. E. Kroon, H. C. Swart, J. J. Terblans, and R. A. Harris, "Photoluminescence of metal-imidazolate complexes with Cd(II), Zn(II), Co(II) and Ni(II) cation nodes and 2-methylimidazole organic linker", *J. Lumin.*, **207**, 454 (2019).
18. R. Li, X. Ren, H. Ma, X. Feng, Z. Lin, X. Li, and C. Hu, "Nickel-substituted zeolitic imidazolate frameworks for time-resolved alcohol sensing and photocatalysis under visible light", *J. Mater. Chem. A*, **2**, 5724 (2014).
19. A. Thamilselvan and R. A. Doong, "Ni-Co bimetallic decorated dodecahedral ZIF as an efficient catalyst for photoelectrochemical degradation of sulfamethoxazole coupled with hydrogen production", *Sci. Total Environ.*, **873**, 162208 (2023).
20. F. P. Addai, J. Wu, Y. Liu, X. Ma, J. Han, F. Lin, Y. Zhou, and Y. Wang, "Amorphous-crystalline phase transition and intrinsic magnetic property of nickel organic framework for easy immobilization and recycling of β-Galactosidase", *Int. J. Biol. Macromol.*, **254**, 127901 (2024).
21. G. Li, G. Xie, C. Gong, D. Chen, X. Chen, Q. Zhang, H. Dong, Y. Zhang, C. Li, J. Hu, Y. Chen, L. Yu, and L. Dong, "Hydrogen-assisted synthesis of Ni-ZIF-derived nickel nanoparticle chains coated with nitrogen-doped graphitic carbon layers as efficient electrocatalysts for non-enzymatic glucose detection", *Microchim. Acta*, **189**, 80 (2022).

22. J. Meng, C. Niu, L. Xu, J. Li, X. Liu, X. Wang, Y. Wu, X. Xu, W. Chen, Q. Li, Z. Zhu, D. Zhao, and L. Mai, "General oriented formation of carbon nanotubes from metal–organic frameworks", *J. Am. Chem. Soc*., **139**, 8212 (2017).
23. X. Zhang, Y. Xu, and B. Ye, "An efficient electrochemical glucose sensor based on porous nickel-based metal organic framework/carbon nanotubes nanocomposite (Ni-MOF/CNTs)", *J. Alloys Compd*., **767**, 651 (2018).
24. D. D. Chronopoulos, H. Saini, I. Tantis, R. Zbořil, K. Jayaramulu, and M. Otyepka, "Carbon nanotube based metal–organic framework hybrids from fundamentals toward applications", *Small*, **18**, 2104628 (2022).
25. M. Thomas, R. Illathvalappil, S. Kurungot, S. Kurungot, B. N. Nair, A. P. Mohamed, G. M. Anilkumar, T. Yamaguchi, and U. S. Hareesh, "Template assisted synthesis of Ni, N co-doped porous carbon from Ni incorporated ZIF-8 frameworks for electrocatalytic oxygen reduction reaction", *New J. Chem*., **44**, 12343 (2020).
26. H. Gao, Y. Liu, M. Ma, E. Meng, and Y. Zhang, "Synthesis of N-doped Co@C/CNTs materials based on ZIF-67 and their electrocatalytic performance for oxygen reduction", *Ionics*, 27, 2561 (2021).
27. G. Singla, S. N. Bhange, M. Mahajan, and S. Kurungot, "Facile synthesis of CNTs interconnected PVP-ZIF-8 derived hierarchically porous Zn/N co-doped carbon frameworks for oxygen reduction", *Nanoscale*, **13**, 6248 (2021).
28. Y. Huang, L. Xie, K. Zhuo, H. Zhou, and Y. Zhang, "Simultaneous catalytic reduction of p-nitrophenol and hydrogen production on MIL-101 (Fe)-based nanocomposites", *New J. Chem*., **45**, 3120 (2021).